EFFECT OF T-SHAPE SPLITTER ON THE HYDRAULIC RESPONSE OF THE BRIDGE PIER

Tahseen Ali JABBAR[1], Rafi Mohammed QASIM[2], Safaa Hameed FAISAL[3*]

The flow around circular pier nearby splitter has T-shape is studied numerically. ANSYS Software/ Fluent is used to perform the hydraulic analysis. Laminar, steady, and incompressible flow are adopted in problem solution with Reynolds number ranging from 40 to 200 to ensure laminar flow with laminar vortex street. The numerical study deals with two major parameters, these parameters are Reynolds number and the horizontal distance between the pier center and rear part of the splitter. The investigation includes the effect of these two parameters on the vortex's length, streamlines, pressure contour, and flow velocity contour. The presence of the splitter leads to the formation of vortices, these vortices are distributed as two vortices at the wake region of the circular pier and two vortices at the region between the rear part of the splitter and the leading part of the circular pier. These vortices are non-symmetrical, also the length and size of these vortices depend mainly on the Reynolds number. It is found from the analysis the disturbance increases with an increase in Reynolds number. The streamlines, pressure field, and flow velocity field are more affected by the horizontal distance between the pier center and rear part of the splitter and in addition Reynolds number will dominate directly the streamlines, pressure field, and flow field. Also, a correlation equation is obtained based on Reynolds number, vortex length, and horizontal distance.

Keywords: Bridge Pier; Splitter; Hydraulic Field; Laminar Flow.

1. Introduction

Nomenclatures:

D	Cylinder diameter	m
L_1, L_2	Total vortices lengths	m
P	Pressure	N/m^2
Re	Reynolds number	-
s	Vortex's length	m
u	x-component of velocity	m/s
v	y-component of velocity	m/s
X	Dimensionless parameters, Eq.(5)	-

[1] Lecturer, Department of Fuel and Energy Engineering, Basra Engineering Technical College, Southern Technical University, Basra, Iraq, e-mail: tahseen.ali@stu.edu.iq
[2] Assis. Prof., Department of Fuel and Energy Engineering, Basra Engineering Technical College, Southern Technical University, Basra, Iraq, e-mail: rafi.mohammed@stu.edu.iq
[3*] Lecturer, Department of Thermal Mechanical Engineering, Basra Engineering Technical College, Southern Technical University, Basra, Iraq, e-mail: s_hfaisal100@stu.edu.iq (corresponding author)

x	Distance between the splitter and the center of the cylinder	m
μ	Viscosity	kg/m.s
ρ	Density	kg/m^3
η	Dimensionless parameters, Eq.(4)	-

Bridge pier is considered an important structural element that transfers the load from the super structure to the bridge foundation, therefore it is very important to seek about the hydraulic response of the pier under hydraulic loading to prevent or avoid hydraulic collapse. This problem represents a challenge to the hydraulic designer and hydraulic engineer owing to direct alteration between hydraulic variables which dominate the problem and hydraulic field response which is surrounded the pier. The desirable solution to this problem is best accomplished by using a splitter. This splitter can reduce the scour depth, turbulent intensity, and flow velocity around the pier and this reduction depend on the location of the splitter with respect to the pier location. The hydraulic interference between the hydraulic field which is surrounded the splitter and the pier respectively is studied numerically by Qasim et al. [1], Jabbar et al. [2]. In these works, the influence of the vane angle on the hydraulic pattern around the pier is investigated. They seek for the following; stream function, strain rate, swirling, flow velocity in the flow direction, vorticity, radial velocity, drag coefficient, distribution of pressure with pressure coefficient, average flow velocity, shear stress, lift coefficient, and coefficient of skin friction. Both of these studies show how the turbulent characteristics are reduced owing to the occurrence of separation processes and dissipation processes along the circumference of the vane and this will be reflected directly on the flow pattern which is surrounded the cylinder. Also, Qasim and Jabbar [3] dealt with the impact of the rectangular vane which is located at the upstream of the cylinder. This study intensified on the static pressure with pressure coefficient, flow velocity, eddy viscosity, and turbulent dissipation rate with kinetic energy and turbulent intensity. The study reveals how the turbulent characteristics can be reduced by using the vane at the upstream of the cylinder. ANSYS software is used to achieve the numerical analysis of the three previous papers. Also, the vane has a vital rule in reducing the scour process around the bridge pier for example Abdulhussein et al. [4] did an experimental study to investigate the impact of using a strip guide panel to reduce the scour around a cylindrical pier. From the obtained results, they found that the scour around the pier with guide panel is less than the scour around the pier without using the guide panel. Also, many papers dealt with problem of the hydrodynamic field around the pier like Jalal and Hassan [5] employed Flow-3D model to study numerically the local scour around the pier of the bridge and compared the numerical results with Melville laboratory experimental model. Kaustubh and Bharat [6] performed numerical investigating by adopting CFD, Eulerian multiphase model, k-epsilon model to study the scour around the pier. The simulation of flow around the pier is achieved in three-dimension, different shapes of the pier are adopted in the numerical study; these shapes are: cylindrical, square, elliptical, and streamlined. Abdulhussein and Qasim [7] collected some experimental data to build three different equations which are employed to predict the scour around the cylindrical pier. These equations depend on the flow field characteristics, pier diameter, and soil particle diameter. Zaw [8] did a comparison between the field observation and numerical simulation for the scour around the bridge pier. Fluent and Gambit software are used for numerical simulation. The findings of numerical simulation and observation are found to be in good agreement. Ramos et al. [9] performed a numerical model that relied on the large eddy simulation to predict the flow pattern around the cylindrical pier in a three-dimension field, the pier is mounted on the fixed and flat bed, this study represents a common case that is pertinent for the investigation of scour and flow around piers of the bridge. Khassaf and Abdulwhab [10] adopted an artificial neural network to predict the depth of local scour around the bridge pier, the laboratory data of some previous papers with the data of this paper were adopted for this study. The scour is investigated under clear water conditions. The main target of this prediction is to estimate the maximum local scour around the pier. Ramos et al. [11] used the OpenFOAM to investigate numerically the flow field around an isolated pier with a circular section. The study dealt with velocity, vorticity, shear stress of the bed, and drag coefficient. The large eddy simulation is adopted to perform the numerical analysis. Khassaf and Shakir [12], investigated the scour around the piers of Al-Kufa Bridge numerically by using HEC-RAS software, also field measurements are collected. The estimated scour depth from HEC-RAS software is compared with the observed data. As well, some researchers dealt with the von Kármán vortex, for example, Gustafsson [13] mentioned when a flow passes the bluff body like a cylinder body the vortex shedding is formed at the rear part of the cylinder consequently the body will vibrate and this is known as a Von Kármán vortex street. Kwon and Choi [14] studied the laminar vortex shedding at the rear part of a circular cylinder with a splitter plate attached to the cylinder. They found that when the splitter plate's length exceeds a critical length, the vortex shedding at the rear portion of a circular cylinder totally vanishes. They also discovered that this critical length is proportional to the Reynolds number. As plate length increases, the Strouhal number of the vortex shedding progressively decreases until the plate length is almost equal to the cylinder diameter. As well, the splitter plate leads to reduce in the net drag. Roussopoulos [15] studied experimentally the detail of vortex shedding from a cylinder that has a circular section at a low Reynolds number by utilizing the feedback to stabilize the wake instability. Experiments have been done both in an open water channel and a wind tunnel with flow visualization. Park et al. [16] reported the feedback control of von Kármán vortex shedding at the rear portion of a circular cylinder when Reynolds numbers are considered small by computational study. In two dimensions they solved numerically the Navier–Stokes equations with feedback.

The objectives of this numerical analysis are:

(a) Find out the interaction between ratio η and ratio X for Reynolds number from 40 to 200.

(b) Find out the interference between Reynolds number and ratio η when ratio X equal to 0.5,1 and 1.5.

(c) Study the streamline at ratio X equal to 0.5,1 and 1.5 when Reynolds number equal to 40,120 and 200.

(d) Study the pressure and flow velocity at ratio X equal to 0.5,1 and 1.5 when Reynolds number equal to 40,120 and 200.

(e) Find a correlation equation comprises Reynolds number, ratio η and ratio X. (the definition of ratio η and ratio X are given in the next text of the paper).

2. Methodology

The two-dimensional hydraulic interaction between an incompressible fluid and pier nearby a splitter is studied. A schematic representation of the hydraulic problem illustrates in Fig. 1. The water flow passes the splitter from the left part and then passes the pier. The flow pattern around the pier is deformed owing to the existence of the T-splitter. Fig. 2 shows the fluid domain size dimensions which are employed to solve the entire hydraulic problem.

The dimensions of the T-splitter arms are equal to the pier diameter. The splitter is located at the pier upstream. The study is based on the different locations x, which is pointed to the horizontal distance measured from the pier center to the downstream of the T-splitter. In the case of $x = D/2$, it means that the splitter has a direct contact with the boundary layer region of the pier. According to Fig. 1, s is pointed to the length of the vortex at the wake region of the pier. The Reynolds number, which is usually adopted in hydraulic analysis, ranges from 40 to 200, to ensure that there is laminar flow. Laminar vortex street happens when Reynolds number range 40<Re<200 [17]. ANSYS-Fluent software is adopted to analysis the steady flow regime. Table 1 illustrates the boundary conditions applied for the entire hydraulic system. The properties of water are taken as $\rho = 997.1$ kg/m^3 and $\mu = 89.05\text{E} - 5\ kg/s.m$

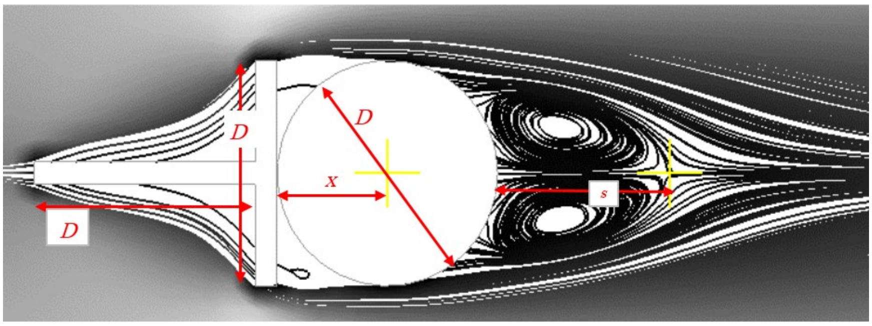

Fig. 1. Hydraulic system problem (flow, T-splitter and pier)

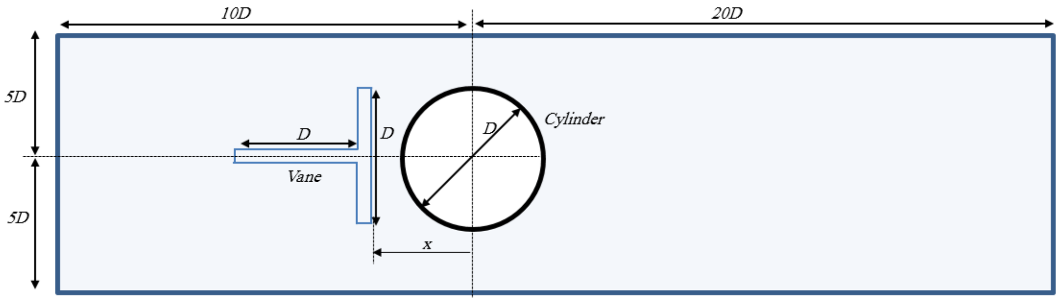

Fig. 2. Problem size domain

Table 1

Hydraulic Problem Boundary Conditions

Location	Type
Inlet	Inlet Velocity
Outlet	Outlet Pressure
Pier and T-Splitter	No-Slip
Channel Bed and Sides	No-Slip

Table 2 shows the total numbers of nodes and elements for various ratios ofx/D. Here, we selected a case that shows a mesh composed of 38903 elements and 39781 nodes, and these mesh details are shown in Fig. 3 with the value of $x = D$

Table 2

The Mesh Details

x/D	Number of nodes	Number of elements	x/D	Number of nodes	Number of elements
0.5	39633	38739	1.1	39578	38701
0.6	39105	38233	1.2	39625	38744
0.7	39334	38460	1.3	39510	38633
0.8	39457	38583	1.4	39566	38684
0.9	39736	38856	1.5	39323	38447
1	38903	39781			

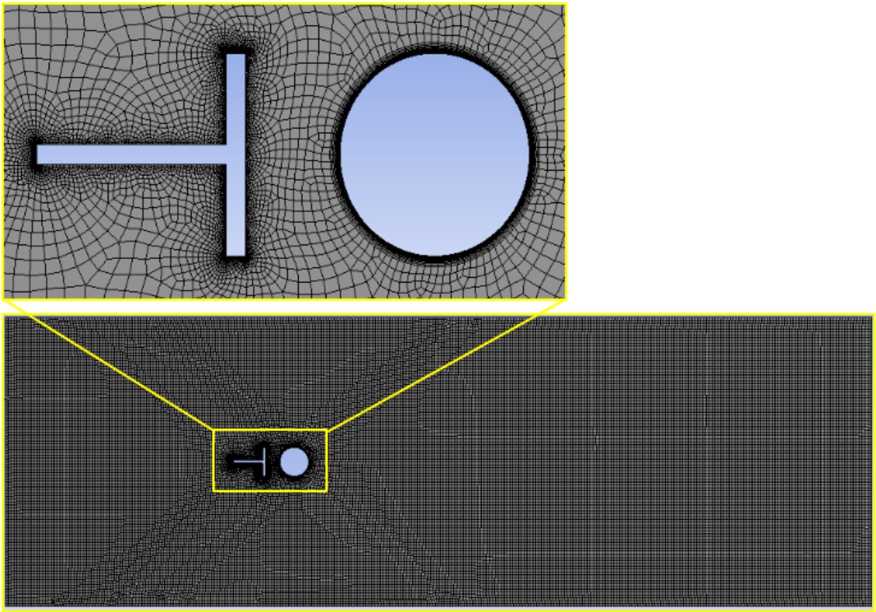

Fig. 3. The mesh of the model (38903 nodes and 39781 elements), $x = D$

The CFD governing equations that will be used for the simulation are the conservation of momentum equation and incompressible fluid continuity equation as given in equations (1) to (3), respectively [18,19].

$$u\frac{\partial u}{\partial x} + v\frac{\partial u}{\partial y} = -\frac{1}{\rho}\frac{\partial P}{\partial x} + \frac{\mu}{\rho}\left(\frac{\partial^2 u}{\partial x^2} + \frac{\partial^2 u}{\partial y^2}\right) \tag{1}$$

$$u\frac{\partial v}{\partial x} + v\frac{\partial v}{\partial y} = -\frac{1}{\rho}\frac{\partial P}{\partial y} + \frac{\mu}{\rho}\left(\frac{\partial^2 v}{\partial x^2} + \frac{\partial^2 v}{\partial y^2}\right) \tag{2}$$

$$\frac{\partial(u)}{\partial x} + \frac{\partial(v)}{\partial y} = 0 \tag{3}$$

The present paper deal with two different non-dimensional ratio the first is η while the second is X:

$$\eta = \frac{s}{D} \tag{4}$$

$$X = \frac{x}{D} \tag{5}$$

Where s: vortex length and D: cylinder diameter.

3. Verification

Before studying the influence of the T-splitter on the hydraulic pattern around the bridge pier, it is very important to test some previous studies to check the validity of the software which is employed to analysis the present problem. The proposed case for a validation procedure is that suggested by Rajani et al. [20], which referred to the analysis of the flow around the cylinder in two dimensions. It is clear that Fig. 4 produces a good comparison between the result obtained from the previous study and the current prediction.

4. Mesh independent

Elements number has a remarkable effect on the flow field around both splitter and pier, so it is essential to use a suitable number of elements to perform the solution. Fig. 5 shows the relation between the number of elements and the ratio η, where η is the ratio between vortex length and the cylinder diameter. It is clear from the figure the ratio remains constant when the numbers of elements become greater than 10000. Fig. 5 is drawn for $Re = 40$ and T-splitter has a direct touch with the pier ($X = 0$).

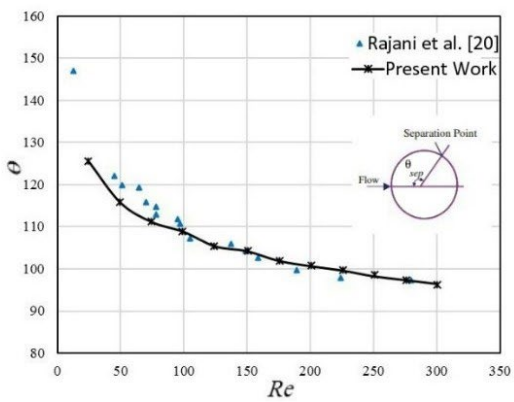

Fig. 4. Relation between Reynolds numbers and separation angle

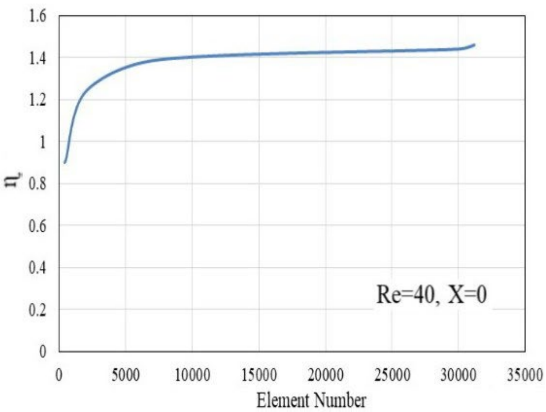

Fig. 5. The adopted mesh independent

5. Results and discussion

The flow around pier represents a noticeable subject and problem at the same time, due to the simultaneous alteration in the flow field around the pier. Therefore, this subject must be considered seriously by the hydraulic designers and engineers. When ratio X increases, ratio η decreases, as seen in Figs. 6(a), 6(b), and 6(c). To put it another way, as the horizontal distance between the pier center and the downstream of the splitter increases, the vortex length in the wake region shrinks. This behavior happens with the different values of Reynolds number. When Reynolds number is increased, the wake region becomes unstable, which should lead to the alteration in the vortex length at the wake region. We have two sorts of separation points in the case of a pier near a T-splitter: the first is mobile points that exist on the cylindrical pier surface, and the second is fixed points that exist on the T-splitter surface. As a result, as the horizontal distance x increases, the position of movable points along the pier's perimeter changes, and this has a direct impact on vortex length in the wake zone.

Fig. 7 depicts the relationship between Reynolds number and ratio η. As Reynolds number increases, the ratio η increases as well. The elongation of vortices in the wake zone increased as the Reynolds number increased. The presence of a T-splitter will also affect the position of separation points around the perimeter of a cylindrical pier, which will be reflected in vortex elongation. It is obvious from the figure when ratio $X = 0.5$, the relation trend is described as linear, while as the ratio X increase the relation become nonlinear.

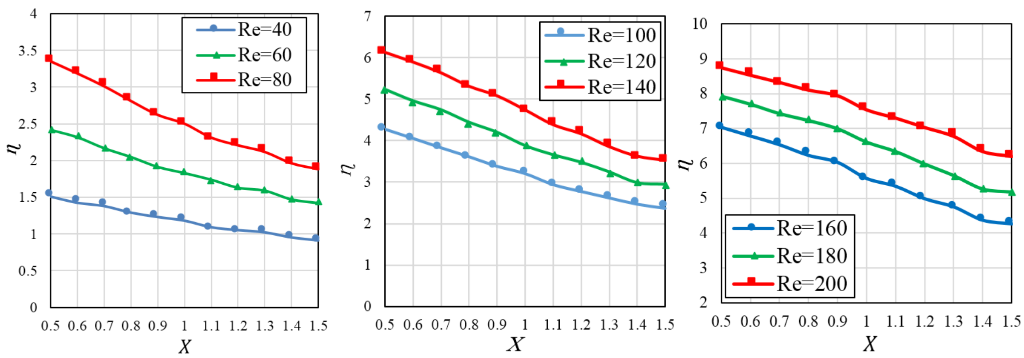

(a) (b) (c)

Fig. 6. Relation between ratio X and ratio η, (a) $40 \leq Re \leq 80$,(b) $100 \leq Re \leq 140$, and (c) $160 \leq Re \leq 200$

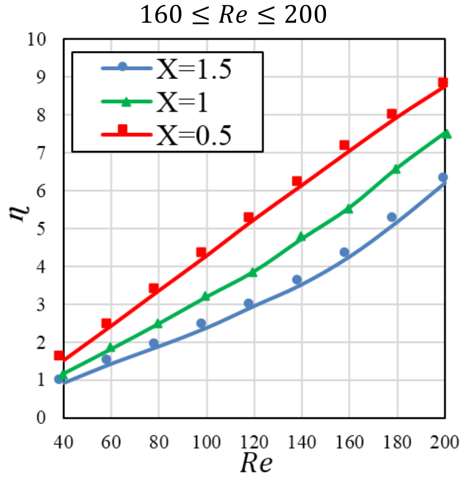

Fig. 7. The effect of splitter position and Re on the vortex length

Figs. 8(a), 8(b), and 8(c) depict the streamline contour for three different values of ratio X for a Reynolds number of 40. Stream line figures give an interesting behavior for the vortex formation in the wake region of the cylindrical pier, in fact, a pair of non-symmetrical vortex will form and grow at the wake region for all values of ratio X. When the splitter is moved away from the cylindrical pier, however, two different vortices emerge and grow in the area between the pier and the splitter. In addition, these vortices are asymmetrical. From inspection in Fig. 8(b), the upstream vortices are seen greater than the downstream vortices (vortices at the wake region), the same behavior is shown in Fig. 8(c). Also, the size of an upstream vortex will be increased, when the horizontal distance between splitter and pier is increasing.

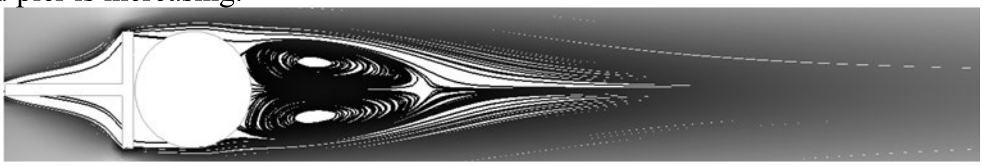

(a)

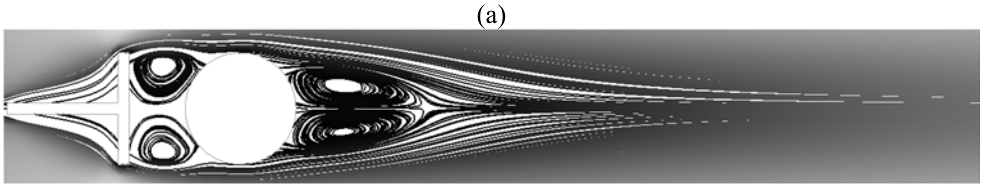

(b)

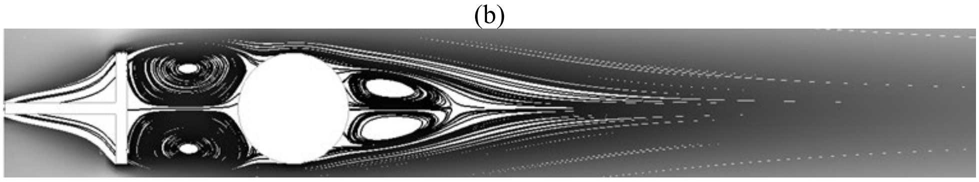

(c)

Fig. 8. Stream lines at $Re = 40$, (a) $X = 0.5$, (b) $X = 1$, (c) $X = 1.5$

Fig. 9 consists of two parts, the first part deal with pressure contour while the second part deals with the flow velocity. The figure is plotted for three different values of ratio X and $Re = 40$. The significant role of T-splitter concentrates on reducing the stagnation pressure at the leading part of the pier, so the stagnation point will be moved (shifted) at the leading part of the T-splitter. Therefore, the presence of the splitter produces active changing in the pressure distribution. Based on the figure, we can be distinguished negative pressure at the leading part of the splitter and the pressure becomes near zero at the rear part of the splitter after that positive pressure will be formed around the cylindrical pier, this positive pressure starts from the boundary layer region and move toward wake region for ratio $X = 1.5$ and in case of gap presence ($X = 1$ and $X = 1.5$) the positive pressure start from the rear part of the splitter and extends toward the wake region of the pier. The T-splitter reduce the stagnation pressure by the friction which develops between flow and the splitter when the flow crosses it, this feature will reflect on the pressure distribution directly. The flow velocity field around the pier nearby T-splitter is influenced by flow separation and dissipation, when the flow passes the splitter, water flow suffers tremendous changes owing to the separation and dissipation process which occurs along the circumference of the splitter. It is clear from the contour that the flow velocity will be increased sharply after the flow crosses the splitter.

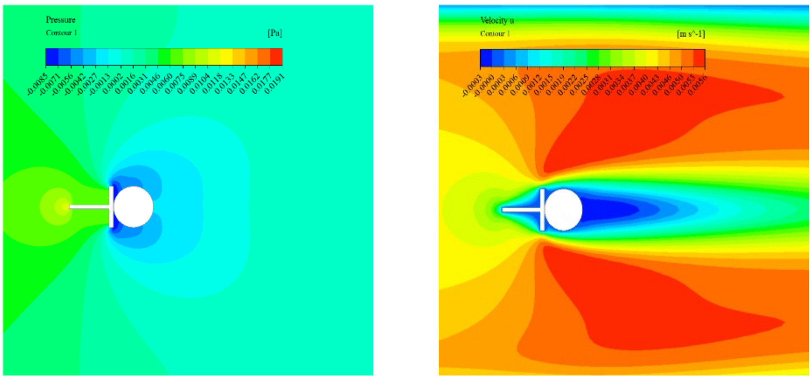

$(a)\ X = 0.5$

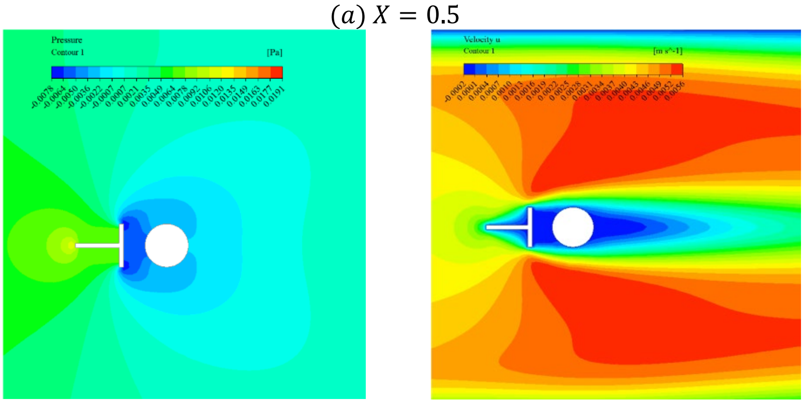

(b) $X = 1$

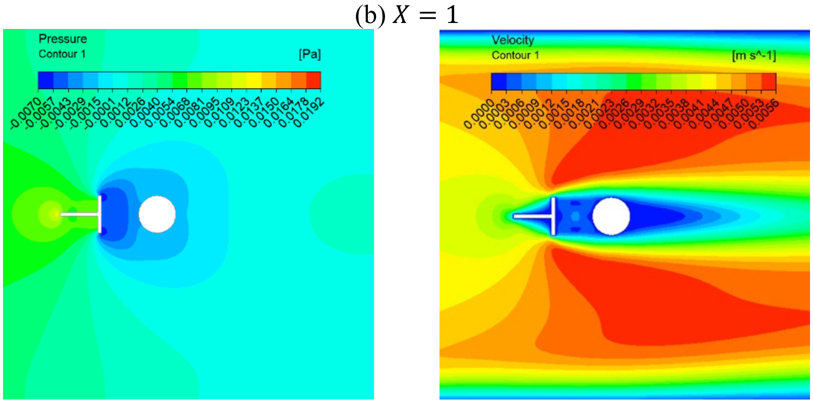

(c) $X = 1.5$

Fig. 9. The pressure and velocity contours at $Re = 40$

As Reynolds number increase the disturbance appear clearly and this will be reflected directly on the vortex's formation and size. This problem appears clearly as seen in Figs. 10(a), 10(b), 10(c), 11(a), 11(b), and 11(c) regardless of the value of ratio X. In general, for all figures the wake region of the pier includes a pair of non-symmetrical vortices, while the region between the rear part of the splitter and leading part of the pier also includes a pair of non-symmetrical vortices, except, when ratio $X = 0.5$ this region will not contain any formation of vortices. It is apparent from all figures when ratio $X = 1$ and $X = 1.5$, the upstream vortices (vortices between splitter and pier) move toward the side of the pier. Also, the length of the vortices at the wake region is greater than the length of vortices in the region between pier and splitter.

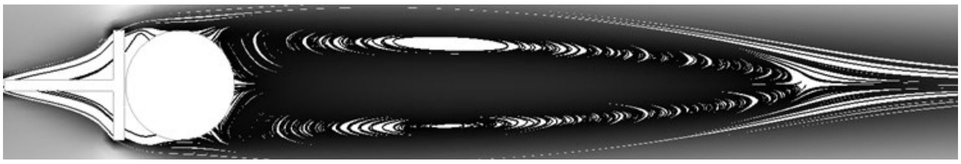

(a)

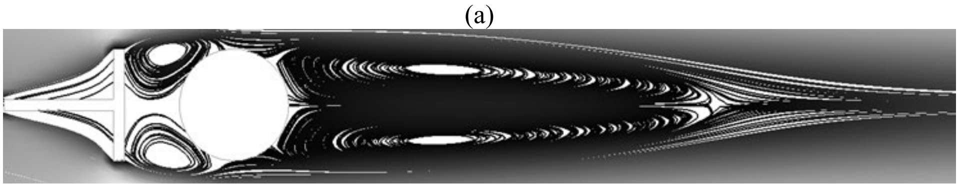

(b)

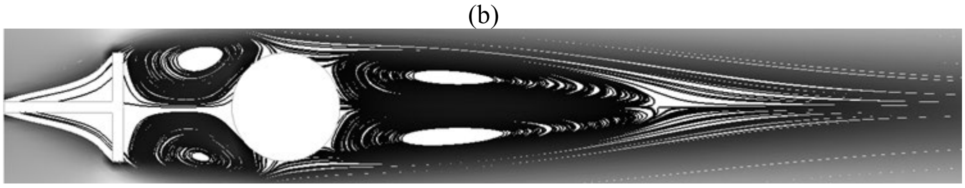

(c)

Fig. 10. Stream lines at $Re = 120$, (a) $X = 0.5$, (b) $X = 1$, (c) $X = 1.5$

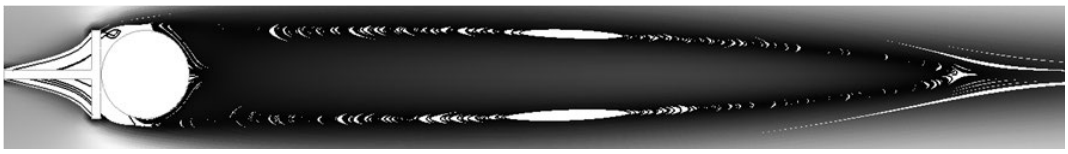

(a)

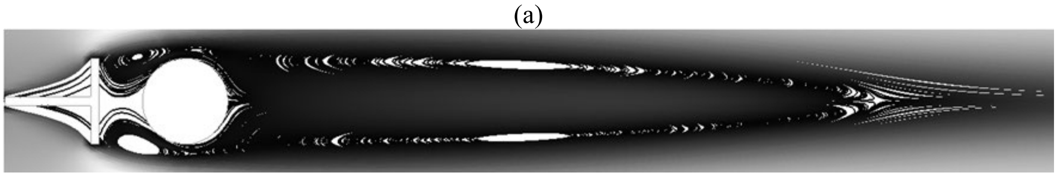

(b)

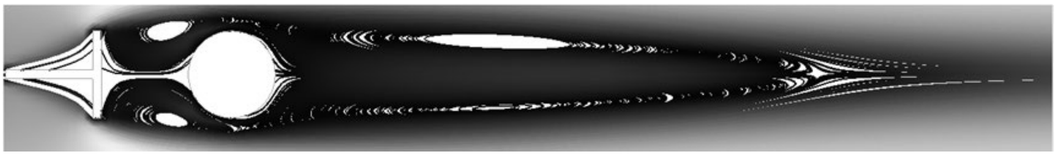

(c)

Fig. 11. Stream lines at $Re = 200$, (a) $X = 0.5$, (b) $X = 1$, (c) $X = 1.5$

Fig. 12 and 13, consist of two parts, the first part deals with pressure contour while the second part deals with the flow velocity. Both Figures are plotted for three different values of ratio X. In Fig. 12, $Re = 120$ while in Fig. 13, $Re = 200$. The same clarification which is explained in the previous text for the Fig. 9 is applicable for both Fig. 12 and 13.

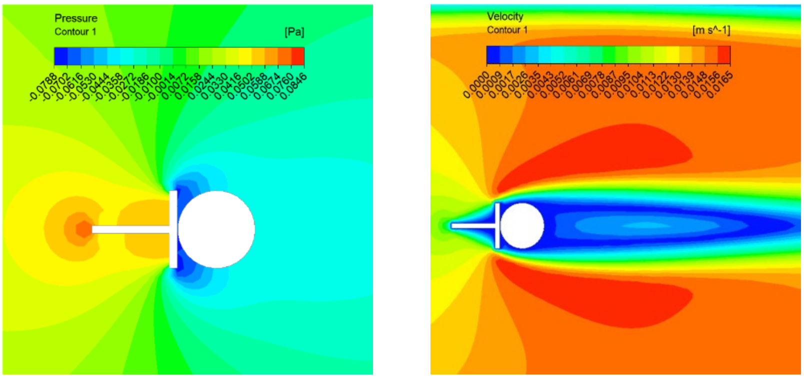

(a) $X = 0.5$

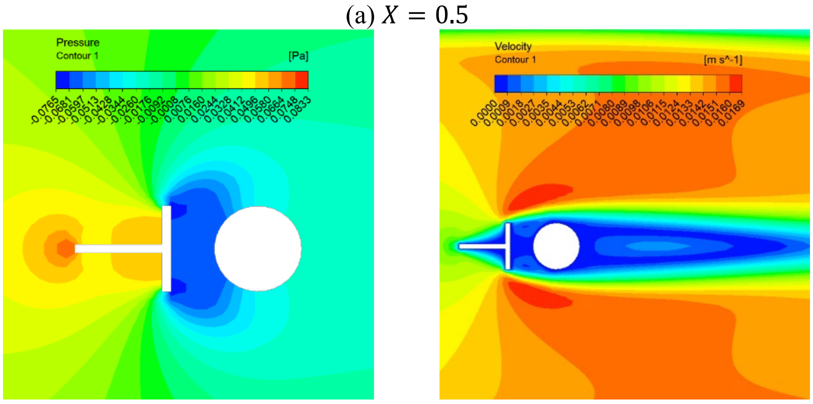

(b) $X = 1$

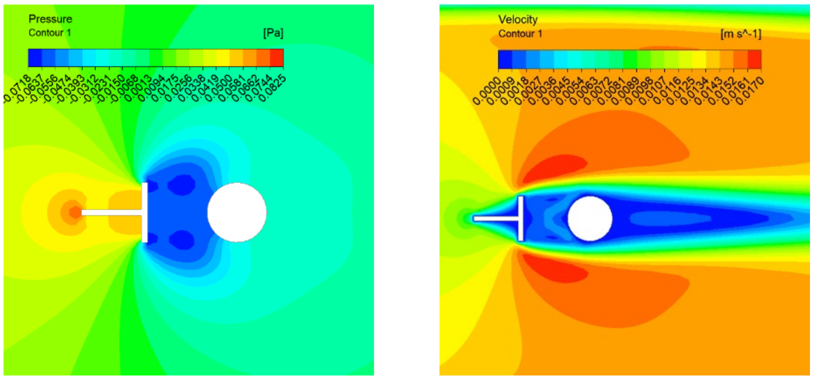

(c) $X = 1.5$

Fig. 12. The pressure and velocity contours at $Re = 120$

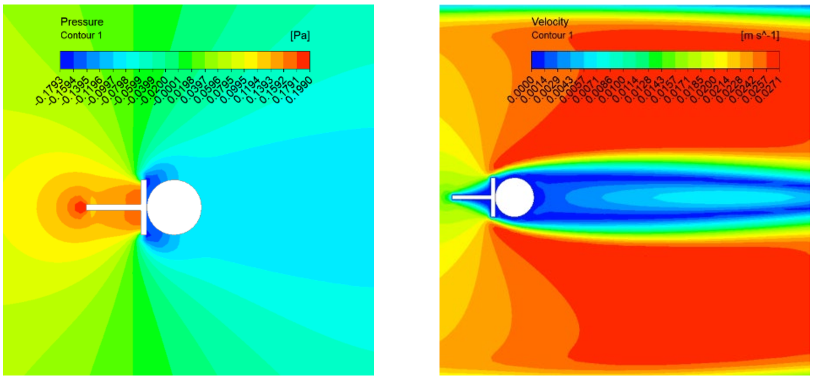

(a) $X = 0.5$

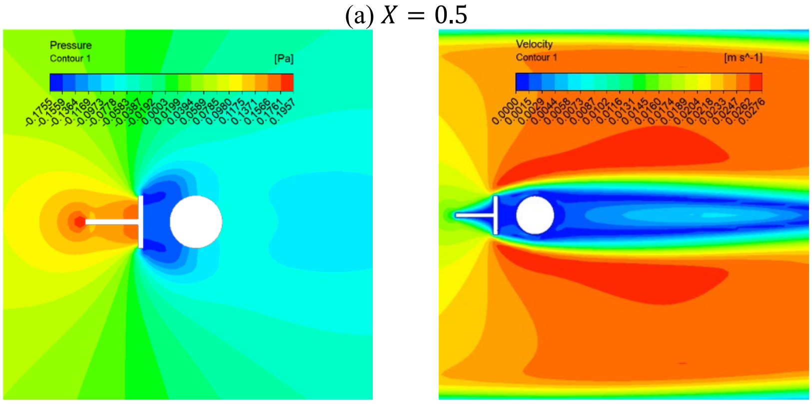

(b) $X = 1$

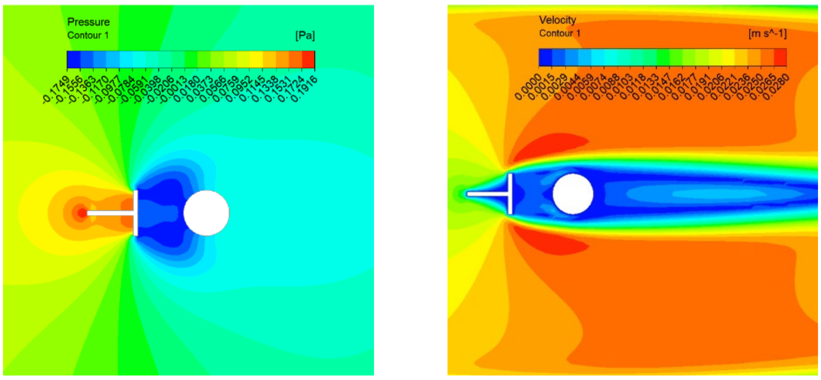

(c) $X = 1.5$

Fig. 13. The pressure and velocity contours at $Re = 200$

The streamlines for different Reynolds number and constant value of ratio X are shown in Fig. 14. With an increase in Reynolds number, the vortices elongation increase at the wake region due to the occurrence of high disturbance. Furthermore, with an increase in Reynolds number the size of vortices increases too. Note that these vortices are non-symmetrical.

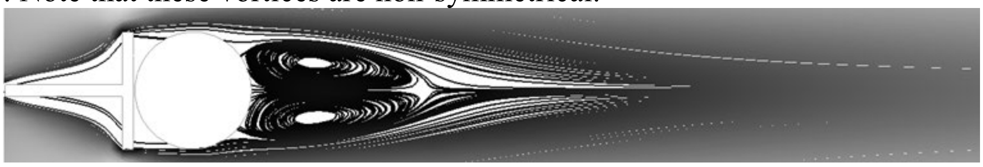

(a) $Re = 40$

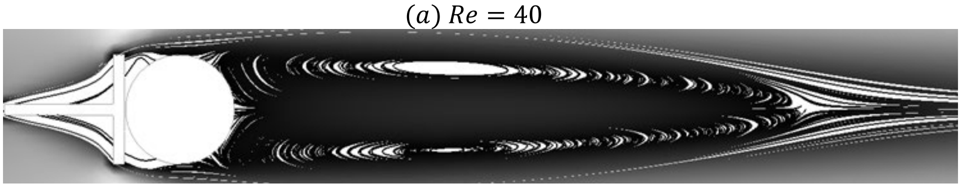

(b) $Re = 120$

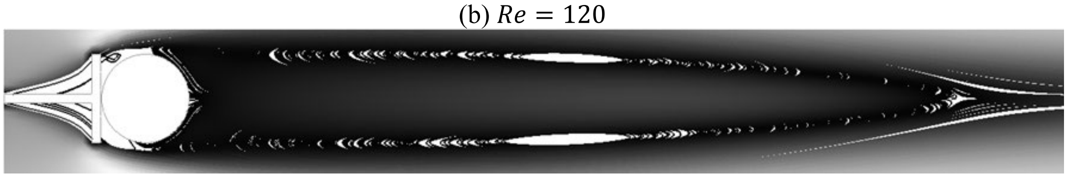

(c) $Re = 200$

Fig. 14. Stream lines at same position of splitter ($X = 0.5$) and different values of Re

The pressure and velocity contours for different Reynolds number and constant value of ratio X are shown in Fig. 15 and Fig. 16 respectively. Both figures show a comparison, considering different values of Reynolds number. Concerning pressure contour, there is no change in pressure distribution and pressure field behavior respectively around pier nearby splitter. The trend is remaining the same where the pressure starts from a negative value and then becomes positive. However, there is a remarkable change in pressure values which have a direct relation with Reynolds number such as the maximum positive pressure is equal to 0.0191 Pa when $Re = 40$, while the maximum positive pressure is equal to 0.0846 Pa when $Re = 120$ and the maximum positive pressure is equal to 0.199 Pa when $Re = 200$. So, we can infer that when the Reynolds number increases the pressure will be increased. For velocity contour, there is no dramatic change in velocity distribution and velocity field behavior respectively around pier nearby splitter. The trend is remaining the same, but there is a noticeable change in velocity values which have a direct relation with Reynolds number such as the maximum positive velocity is equal to 0.0056 m/s when $Re = 40$, while the maximum positive velocity is equal to 0.0165m/s when $Re = 120$ and the maximum positive velocity equal to 0.0271m/s when $Re = 200$so we can infer when Reynolds number increase the velocity will be increased. Ultimately, we can say that the value Reynolds number dominated on the both field of flow velocity and pressure. From the numerical study, we obtain a correlation equation that comprises Reynolds number, ratio η, and ratio X. This equation is considered nonlinear with $R^2 = 0.989$.

$$\eta = A\, Re^B\, X^C = 0.01406 Re^{1.177} X^{-0.4109} \tag{6}$$

Applicable for $40 \le Re \le 200$ and $0.5 \le X \le 1.5$

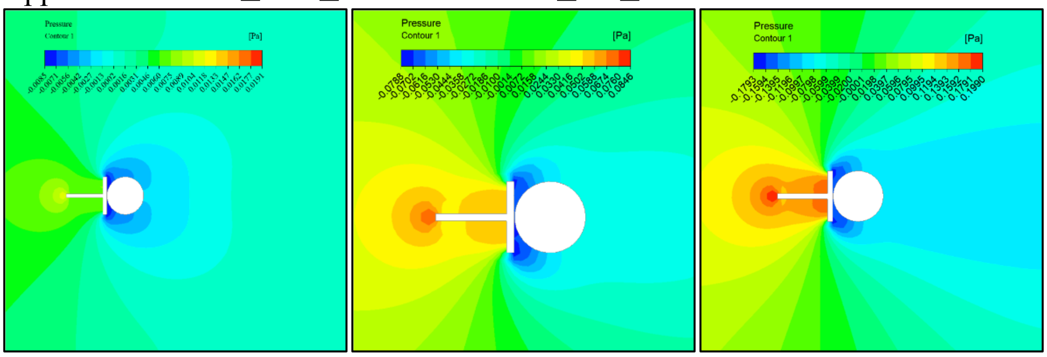

(a) $Re = 40$ (b) $Re = 120$ (c) $Re = 200$

Fig. 15. The pressure contours at same position of splitter ($X = 0.5$) and different values of Re

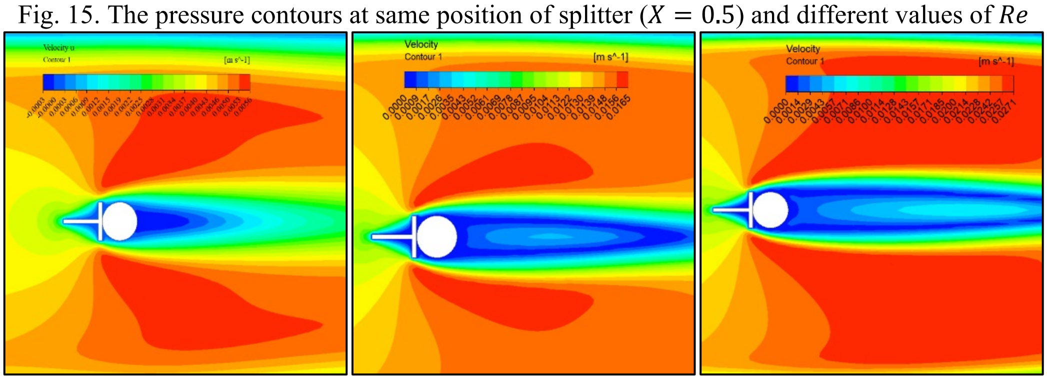

(a) $Re = 40$ (b) $Re = 120$ (c) $Re = 200$

Fig. 16. The velocity contours at same position of splitter ($X = 0.5$) and different values of Re

Fig. 17 shows that both vortices which are grown and developed at the wake region of the pier are non-symmetrical due to their difference in length L_1, L_2. This inference is appeared clearly for all adopted Reynolds numbers in this paper, regardless of the location of splitter from the front face of the pier.

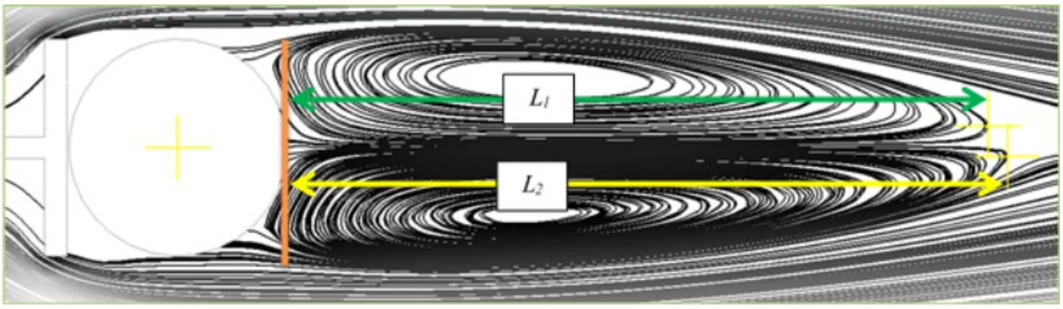

Fig. 17 The vortex lengths at downstream of the pier

6. Conclusions

All of the water hydrodynamic fields produce a huge alteration in the hydraulic field around any obstacle, especially around cylindrical bridge piers, and this alteration will be concentrated on the streamlines, pressure field, and velocity field. To treat this problem, the use of a splitter is adopted to reduce the huge alteration in the hydraulic field. One of the benefits of the T-splitter is that the stagnation pressure will be transferred from the leading part of the pier to the leading part of the splitter, and this mitigates the pressure at the front face of the pier. Unfortunately, this benefit leads to a negative aspect, which is the decrease in the static pressure leads to an increase in the flow velocity around the pier. This T-splitter affects the disturbance at the wake region, especially on the streamlines because of the changing in velocity and pressure. In this simulation, the Reynolds number represents a good indicator to describe the flow disturbance and the disturbance depends mainly on the flow velocity, so we can infer that Reynolds number has an important impact on the streamlines. From the numerical investigation, the following important remarkable aspects are found. The horizontal distance between the pier center and the rear part of the T-splitter has directly impacts on the vortex's length and size. Also, Reynolds number has a direct impact on the vortex length and size, as well both Reynolds number and horizontal distance are responsible for the formation of the vortices especially the vortices between the leading part of the pier and the rear part of the splitter.

REFERENCES

[1]. *Qasim, Rafi, Tahseen Jabbar, and Ihsan Abdulhussein.*, “Flow Field Simulation Between Angle Vane and Cylinder”, Proceedings of 2nd International Multi-Disciplinary Conference Theme: Integrated Sciences and Technologies, *IMDC-IST 2021*, 7-9 September 2021, Sakarya, Turkey, 2022. doi:10.4108/eai.7-9-2021.2315181.

[2]. *Jabbar, Tahseen, Rafi Qasim, and Bassam Mohammed.*, “The Impact of the Vane Angle on the Hydraulic Behaviour Around the Cylinder”, Proceedings of 2nd International Multi-Disciplinary Conference Theme: Integrated Sciences and Technologies, IMDC-IST 2021, 7-9 September 2021, Sakarya, Turkey, 2022. doi:10.4108/eai.7-9-2021.2315298.

[3]. *QASIM, Rafi M., and Tahseen Ali JABBAR.* “An Analytic Study of the Effect of a Vane on the Hydraulic Field Around a Cylinder”, INCAS BULLETIN, **vol**.13, no. 3, September 2021,: pp.123–139. doi:10.13111/2066-8201.2021.13.3.11.

[4]. *Abdulhussein, Ihsan A., Rafi M. Qasim, and Khalid Al-Asadi.*, “Pier Scouring Reduction Using a Strip Guide Flow Panel Device”, RUDN Journal of Engineering Researches, **vol.**20, no. 3 ,December 2019, pp 229–235. doi:10.22363/2312-8143-2019-20-3-229-235.

[5]. *Jalal, Halah Kais, and Waqed H. Hassan.*, “Three-Dimensional Numerical Simulation of Local Scour Around Circular Bridge Pier Using Flow-3D Software”, IOP Conference Series: Materials Science and Engineering, **vol**.745, 2020. doi:10.1088/1757-899x/745/1/012150.

[6]. *Kaustubh, C., and Bharat, J.*, " CFD simulation of local scouring around bridge pier", International Journal of Engineering and Advanced Technology (IJEAT), **vol.**9, no.1, 2019.

[7]. *Abdulhussein, I.A., and Qasim, R.M.*, "Determination of local scour depth of prototype cylindrical pier using physical model data collection", International Journal of Civil Engineering and Technology (IJCIET), **vol**. 9, no. 9, 2018,pp.1283-1301.

[8]. *Zaw, M.T.*, "Analysis of Bridge Pier Scour by Using Numerical Simulations with FLUENT", Int. J.of Research in Chemical, Metallurgical and Civil Eng. (IJRCMCE), **vol**. 5, no.1 ,2018.

[9]. *Ramos, P.X., Maia, L., Schindfessel, L., Mulder, T.De., and Pêgo, J.P.*, "Large Eddy Simulation of the water flow around a cylindrical pier mounted in a flat and fixed bed", 6th International junior researcher and engineer workshop on hydraulic structures, 2016.

[10]. *Khassaf, S.I., and Abdulwhab, A.Q.*, "Modeling of Local Scour Depth Around Bridge Piers Using Artificial Neural Network", Adv. nat. appl. sci., **vol**.10, no.11, 2016,pp. 71-78.

[11]. *Ramos, P., Pêgo, J.P., and* Maia, R., "Numerical simulation of the flow around a pier using openfoam", 3rd . IAHR Europe Congress, Book of Proceedings, Porto – Portugal,2014.

[12]. *Khassaf, S.I.,and Shakir, S.S.*, "Modeling of local scour around al-kufa bridge piers", International Journal of Advance Research (IJOAR), **vol**. 1, no.8,2013.

[13]. *Gustafsson, A*., "Analysis of Vortex-Induced Vibrations of Risers", Master's Thesis in Applied Mechanics, Department of Applied Mechanics, Division of Material and Computational Mechanics Chalmers, University of Technology Gothenburg, Sweden, 2012.

[14]. *Kwon, K., and Choi, H.,* "Control of laminar vortex shedding behind a circular cylinder using splitter plates", Physics of Fluids, **vol.** 8, no.2, 1996, pp.479-486.

[15]. *Roussopoulos, K*., “Feedback control of vortex shedding at low Reynolds numbers”, J. Fluid Mech., **vol.**248, 1993, pp.267-296. https://doi.org/10.1017/s0022112093000771.

[16]. *Park, D. S., Ladd, D. M., and Hendricks, E. W.,* "Feedback control of von Kármán vortex shedding behind a circular cylinder at low Reynolds numbers", Physics of Fluids, **vol.**6, no. 7, 1994, pp.2390-2405. https://doi.org/10.1063/1.868188.

[17]. *Sumer, B.M.,and Fredsoe, J.*, "Hydrodynamics around cylindrical structures", Advanced Series on Ocean Engineering, **vol**. 26, 2006.

[18]. *Dahkil, S. F., Gabbar, T. A., and Jaber, D. K.*, "Numerical Study of The Initial Pressure and Diameters Ratio Effect on The Jet Ejector Performance", Basra J. Eng. Science, **vol**. 14, no. 1,2014,pp.122-135.

[19]. *Sharma, B.,and Barman, R. N.*, "Steady laminar flow past a slotted circular cylinder", Phys. Fluids, 32, 073605, 2020. doi: 10.1063/5.0007958.

[20]. *Rajani, B.N., A. Kandasamy, and Sekhar Majumdar*, “Numerical Simulation of Laminar Flow Past a Circular Cylinder”, Appl. Math. Model., **vol.**33, no. 3, March 2009, pp. 1228–1247.